Pharm Res (2015) 32:403–413
DOI 10.1007/s11095-014-1470-8

RESEARCH PAPER

Fetal Membrane Transport Enhancement Using Ultrasound for Drug Delivery and Noninvasive Detection

Lior Wolloch • Aharon Azagury • Riki Goldbart • Tamar Traitel • Gabriel Groisman • Mordechai Hallak • Joseph Kost

Received: 30 March 2014 / Accepted: 24 July 2014 / Published online: 31 July 2014

ABSTRACT

Purpose The purpose of this research was to evaluate the effect of ultrasound on mass transport across fetal membrane for direct fetal drug delivery and sensing of the amniotic fluid in a noninvasive manner.

Methods Post-delivery human fetal membranes (chorioamnion) were used for *in vitro* experiments, in which the effect of ultrasound on transport across fetal membrane of fluorescent model molecule (250 kDa) was evaluated. *Ex vivo* experiments were carried out on a whole rat amniotic sac. The model molecule or alpha-fetoprotein was injected into the amniotic sac through the placenta. Transport of these molecules across pre- and post-insonation of the amniotic sac was evaluated. The ultrasound enhancement's mechanism was also assessed.

Results The greatest enhancement in mass transport (43-fold) *in vitro* was achieved for 5 min of insonation (20 kHz, 4.6 W/cm^2, 5 mm distance). *Ex vivo* results showed a rapid increase (23-fold) in mass transport of the model molecule and also for alphafetoprotein following 30 s of insonation (20 kHz, 4.6 W/cm^2, 5 mm distance).

Conclusions Mass transport across fetal membranes was enhanced post-insonation both *in vitro* and *ex vivo* in a reversible and transient manner. We suggest that exterior (to the amniotic sac) ultrasound-induced cavitation is the main mechanism of action.

KEY WORDS cavitation · fetal membranes · mass transport · prenatal care · ultrasound

ABBREVIATIONS

FITC	Fluorescein isothiocyanate
PBS	Phosphate buffered saline
s.e.m.	Standard error of mean
SATP	Spatial average temporal peak
SD	Sprague–Dawley
SPTP	Spatial peak temporal peak
US	Ultrasound
αFP	Alpha-fetoprotein

L. Wolloch · A. Azagury · R. Goldbart · T. Traitel · J. Kost (✉)
Ben-Gurion University of the Negev, Beer-Sheva, Israel
e-mail: kost@bgu.ac.il

G. Groisman · M. Hallak
Hillel Yaffe Medical Center, Hadera, Israel

INTRODUCTION

Drug delivery and noninvasive sensing have been the focus of many studies, one aspect of which is prenatal diagnosis. The aim of prenatal diagnosis is identifying structural or functional abnormalities in the developing fetus (1). The common clinical invasive prenatal diagnostic tests used today are chorionic villus sampling and amniocentesis, which have the advantage of high accuracy but carry definite risk to the mother and fetus (2). Therefore, it is of interest to develop noninvasive procedures to extract amniotic fluid samples. In recent years, great progress was made in prenatal genetic diagnosis by analyzing maternal blood, specifically cell-free fetal DNA (cfDNA) (3, 4). A recent study reviewed the clinical validation of maternal blood cfDNA analysis in screening for aneuploidies (5). The study lists three main limitations for implementation of this method. The limitations are the 1–2 weeks needed for the results to be returned (due to the small sample size) and the 1–5% rate of failure to provide results, again due to the small sample size. Also due to the small sample size, some fetal diseases cannot be detected or the accuracy for the detection of these diseases is reduced. Thus acquiring greater concentrations and variety of cfDNA may improve the accuracy and applicability of utilizing cfDNA for detection of fetal abnormalities.

The fetal membranes comprise three distinct layers: The inner layer is the amnion, which provides almost all of the tensile strength of the fetal membranes (6). The outer layers are the chorion laeve (nonvascular tissue) and the decidua

capsularis (7). In general, the sac surrounding the fetus does not develop intact all at once but rather in stages and layers over weeks, somewhat similar to two balloons gradually being inflated inside of a rigid sphere. The final arrangement of membranes is present for at least the last half of the pregnancy. While the chorion is a moderately organized tissue without blood vessels (less organized than skin), the amnion is composed mainly of fibrillar collagen (8)]. The chorion thickness is 431 ± 113 μm, amnion 111 ± 78 μm (skin is 1,000–1,500 μm) (9, 10). The higher organization and thickness of skin may explain why the skin possesses a greater barrier for mass transport.

Sonophoresis is the transport of drugs through intact skin or other biological membranes under the influence of ultrasound (11). Ultrasound at various frequencies has been used to enhance skin permeability (12–16) for non-invasive transdermal drug delivery (17–23) and transdermal monitoring (24–27) in *in vitro*, *in vivo*, and clinical studies. The proposed mechanisms described for this phenomenon are inertial cavitations (and induced acoustic streaming) in the ultrasound's coupling medium (28, 29), and rectified diffusion inside the skin layers (30).

The aim of this work was to investigate the enhancement effect of ultrasound on the transport of molecules through the fetal membranes (in both directions). This potential method has the potential to be used as a means for non-invasive direct fetal drug delivery to the amniotic sac, such as digoxin (781 Da). Another option is administering biological agents such as teraiodothyronine (776.9 Da) for the treatment of fetal hypothyroidism, or as an additional or alternative option for invasive prenatal tests used today. Another possible application may be a non-invasive amniotic fluid extraction for analysis and diagnosis of genetic disorders or other birth defects in the fetus, using a special ultrasound vaginal probe.

MATERIALS AND METHODS

In vitro Transport Experiments

Post-delivery human placentas were received from the Hillel Yaffe Medical Center (authorized by the Center IRB committee). The fetal membranes were cut approximately 1 cm from the placental disc. Later, the membranes were cut into 5 cm×5 cm pieces, cleaned with PBS (Phosphate Buffered Saline, 0.01 M phosphate and 0.137 M NaCl; Sigma-Aldrich), and stored frozen (−20°C) until use (transport and histopathological experiments of fresh unfrozen fetal membranes yielded the same results as frozen; results not shown). Prior to each experiment, the membranes were removed from the freezer and thawed at room temperature for 20 min, followed by an additional cleaning with PBS (stirring in 100 mL for 20 min).

Fetal membrane permeability was evaluated by measuring the transport rate of fluorescent conjugated molecules – FITC-Dextran (Fluorescein Isothiocyanate-Dextran, Mw of 4, 40, and 250 kDa; Sigma-Aldrich). The experiments were performed in glass diffusion cells composed of 8.5 mL donor and 5.5 mL receiver compartments with a transport cross-section area of 2.27 cm^2. The integrity of each membrane sample was evaluated visually, prior to and after the experiments. The two compartments were separated by membranes mounted with the amnion membrane facing the donor compartment (lower compartment, mimicking the embryonic compartment, see Fig. 1b). It should be noted that transport experiments where the chorion was facing the donor chamber yielded similar results (results not shown).

The donor compartment was filled with 0.5 mg/mL solution of FITC-Dextran dissolved in PBS (pH 7.4), while the receiver compartment was filled with PBS (pH 7.4) in the coupling medium. The diffusion cells were protected from light (in order to eliminate photo bleaching) and placed in an orbital shaker at 100 rpm and temperature of 37°C. Samples of 1 mL each were withdrawn from the receiver compartment at different time intervals, and replaced by 1 mL of fresh 0.01 M PBS. Later, these samples were analyzed to determine the concentration of the fluorescent labeled Dextran.

Ultrasound Application

Ultrasound probe (VCX-400, Sonics & Materials, Newton, CT, USA, with a frequency of 20 kHz and a 13 mm probe) was located in the receiver compartment and immersed in the

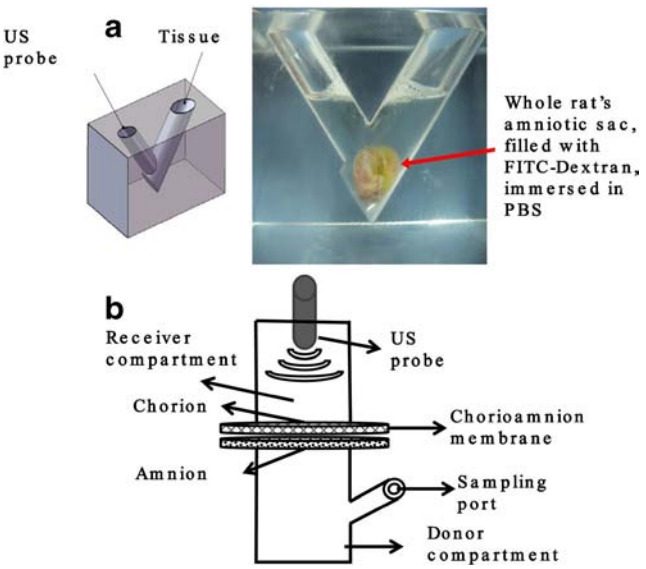

Fig. 1 (**a**) *Ex vivo* experimental set-up – schematic drawing of the experimental chamber (*left*), and a photo of a whole rat amniotic sac, filled with FITC-Dextran, immersed in PBS, located inside the release chamber (*right*). (**b**) *In vitro* experimental set-up.

fluid that also served as a coupling medium. Different intensities and application times were evaluated. In order to minimize thermal effects, a 50% duty cycle application was chosen (1 s on, 1 s off).

FITC-Dextran Analysis

The FITC-Dextran concentration was determined using a fluorescence plate reader (Infinite M200/Tecan™ Austria GmbH). The fluorescence intensity was measured at 490 nm excitation and 520 nm emission wavelengths. The concentrations were calculated from the fluorescence intensity, based on a preprepared calibration curve. For each evaluated parameter, 3–5 independent repetitions (from different human sources) were performed. When the concentration was below the detection limit, the detection limit concentration was used (i.e. the enhancement effect calculated was lower than should be).

Ex Vivo Transport Experiments

Ex vivo transport experiments were carried out on a whole amniotic sac (i.e., including the embryo), which was removed from 12 to 13 days pregnant euthanized Sprague–Dawley (SD) rats, received from the Ben-Gurion University vivarium and adhered to the "Principles of Laboratory Animal Care" (NIH publication #85-23, revised in 1985). All animal procedures were approved by the University Institutional Animal Care and Use Committee.

SD rats were anesthetized with 0.25 mL Ketastet (100 mg/mL, Ketamine HCl Inj., USP; Fort Dodge Animal Health, Iowa, USA) and 0.1 mL XYL-M (20 mg/mL, Veterinary Xylazine; VMD, Arendonk, Belgium) and later euthanized by 2 mL of Pentobarbitone (200 mg/mL, Pental veterinary injection; CTS Chemical Industries Ltd., Israel), all injected intramuscularly. The abdomen of the euthanized rat was opened and the amniotic sacs were removed from the uterus using surgical scissors.

Transport Experiments with a Model Molecule

FITC-Dextran was used first as a model molecule. In order to simulate conditions similar to those in the *in vitro* experiments, the same initial FITC-Dextran concentration in the amniotic sac (0.5 mg/mL) was used. The amniotic fluid volume was measured several times in SD rat amniotic sacs in this pregnancy stage, and was found to be 0.5 mL. Therefore, 0.2 mL of 1.75 mg/mL FITC-Dextran was injected into the amniotic sac through the placenta (avoiding puncturing of the embryo), using a 27 gauge needle attached to 1 mL syringe. After solution injection was complete, the needle was withdrawn gently, and the penetration point of the needle was sealed, using fast acting glue (MUNIX, 3 g, India).

The amniotic sac was placed in a chamber filled with 15 mL of PBS (see Fig. 1a), where the ultrasound probe (S-4000 Astrason® Ultrasonic Processor, Misonix Inc., NY, USA, with a frequency of 20 kHz and a 13 mm probe) was applied at different distances and intensities for 30 s in a continuous mode. The chamber was protected from light (to avoid photo bleaching), and placed in an orbital shaker at 100 rpm and temperature of 37°C. Samples of 1 mL each were withdrawn from the chamber's medium at different time intervals, and replaced by fresh 0.01 M PBS. Later, these samples were analyzed in order to determine the concentration of the fluorescent molecule.

Transport Experiments with Alpha-Fetoprotein (αFP)

200 μL of 15 ng/μL αFP solution (Alpha fetoprotein, 63 kDa, Purified Human Alpha Fetoprotein/AbD; Serotec, UK) dissolved in 0.01 M PBS were injected, in a similar manner to FITC-Dextran, into the rat amniotic sac. The resulting concentration of αFP in the amniotic sac was 4.3 ng/μL. From this point on, the experiment was identical to the *ex vivo* FITC-Dextran experiment. The samples taken from the receiver chamber were analyzed using a commercial ELISA kit (Active® AFP ELISA/DSL-10-8400; Diagnostic Systems Laboratories Inc., TX, USA).

Histology

Post-delivery human fetal membranes from different *in vitro* transport experiments were delivered for histology analysis; 9 μm thick paraffin sections were prepared from each sample and stained with Hematoxylin and Eosin. The sections were later viewed and imaged by light microscope (BX51; Olympus, Tokyo, Japan). All photographs were taken at 4× and 40× magnifications using a CCD camera (DP70, Olympus, Tokyo, Japan) attached to the microscope.

Statistical Analysis

All the data represent the mean and standard error of mean (s.e.m.) of 3–5 independent repetitions; each repetition was performed on a tissue from a different biological source. Statistical significance was analyzed by student *t*-test. Differences were considered statistically significant when $p<0.05$.

RESULTS AND DISCUS?SION

In Vitro Transport

Preliminary results obtained in our lab demonstrated large differences in transport properties of fetal membranes from

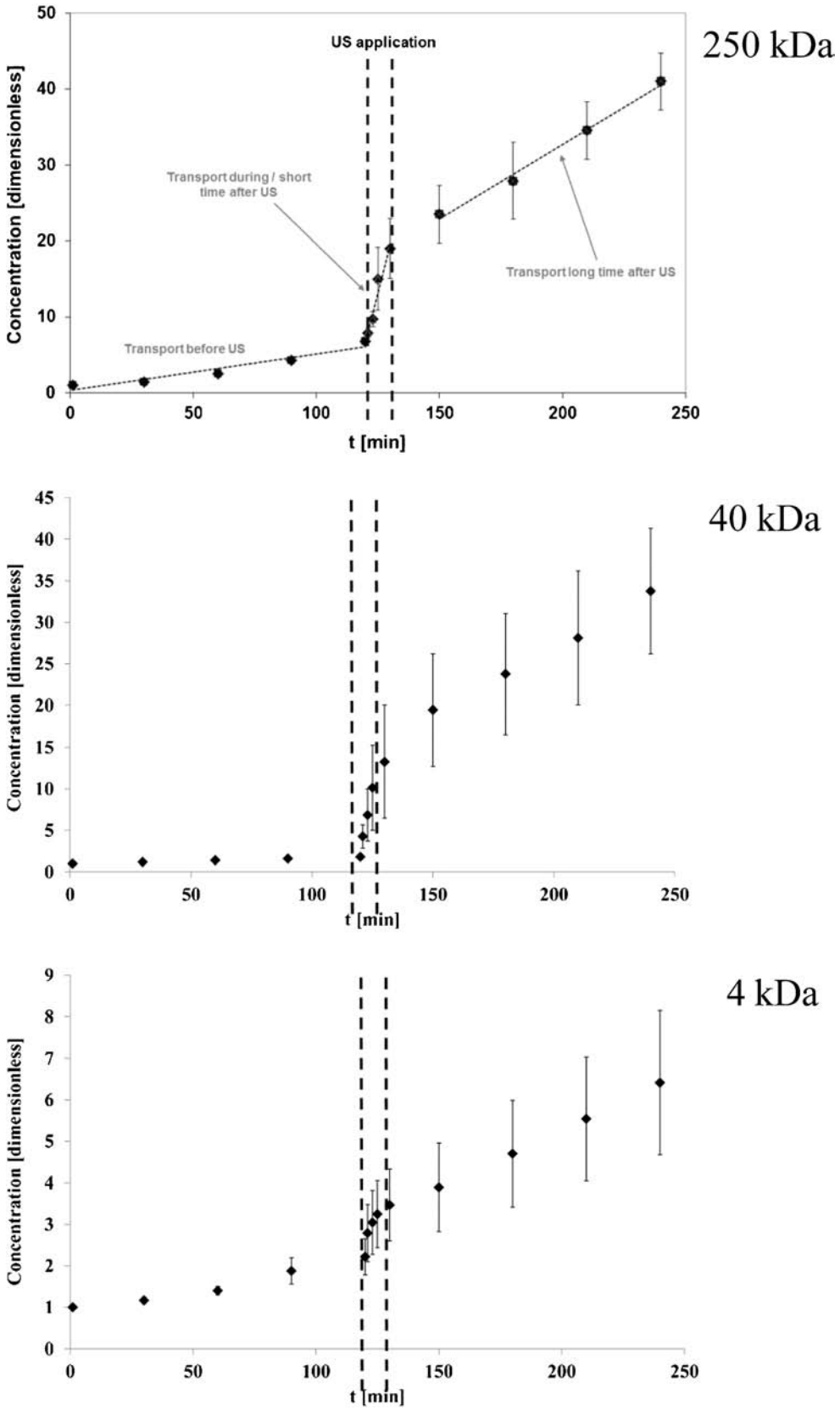

different and even the same human source. Therefore, in our experimental setup, all of the concentration measurement points presented in the figures were normalized by dividing the concentration values by the initial

◀ **Fig. 2** Transport profile of FITC-Dextran (250, 40, and 4 kDa) through post-delivery human fetal membranes. Data points represent mean ± standard error (s.e.m.) of 3–5 identically conducted experiments, each from a different biological source. The three slope regions used for transport enhancement calculations: (1) before US (calculated by 5 measurement points taken during a period of 120 min), (2) during/short time after US (calculated by at least 3 samples taken during or a short time (up to 10 min) after ultrasound application), and (3) long time (30–90 min) after US (at least 4 samples).

concentration, taken after 1 min of transport through the same membrane.

Preliminary Diffusion Experiments Through the Fetal Membranes

In order to evaluate the potential for mass transport (normalized quantity passed/time) enhancement by ultrasound, we initially studied the passive diffusion of fluorescent molecules through the membranes. We found that fetal membranes significantly differ in their permeability properties as was also implied by Nishida *et al* (31). Thus, we decided to perform the *in vitro* experiments by first measuring the passive diffusion of each membrane (base-line), followed by ultrasound application (we also found in our preliminary experiments that the membrane-increased transport effect reversed quite rapidly; therefore pretreatment as used for skin cannot be applicable here) (18, 32, 33). The transport enhancement was calculated in comparison to the base-line permeation of each membrane. In order to do so, the slopes of three regions in the concentration *vs.* time profile were calculated (Fig. 2) as follows: (1) Before ultrasound (US) application – the slope of this region establishes the base-line transport, (2) During/short time after US application, and (3) Long time after US application. All slopes were calculated with the linear regression function using Excel™ software with minimum R^2 value of 0.90. As can be seen in Fig. 2, there is a 7, 1.8, and 2.2-fold (for 250, 40, and 4 kDa respectively) increase in concentration after 120 min (compared to 1 min concentration) during passive transport. These results imply that the fetal membranes are permeable to FITC-Dextran (4–250 kDa) in a passive manner. Also seen in Fig. 2, the major enhancement occurs during and a short time after ultrasound application (for all three Mw tested), while it decreases a long time after sonication – the slopes for the "during/short time after US" are steeper than the slopes for the "long time after US" (for all three Mw tested); thus the transport rate is decreasing after a short time, indicating a reversibility in the effect on the membranes. This phenomenon is in contrast to what is known for skin (where ultrasound application induces a transport enhancement that lasts for up to 24 h) (18, 24, 25). The greater slope after US application (compared to the slope before US application) may suggest structural modification of the fetal membranes. However the results of the histopathological test (shown later in histology analysis subheading) do not support non reversible structural modification. For longer permeability experiments (results not shown) the fetal membranes mass transport rate has reversed back to its initial rate (pretreatment) indicating the effect on the fetal membranes is reversible (as with skin). Finally, the greater error bars observed for the US application (during and after) compared to the passive transport may be explained by the known heterogenic nature of US effect on membranes (2, 34).

Ultrasound Intensity and Application Time

Since no prior information on the effect of low frequency ultrasound on transport enhancement of fetal membrane was found in the literature, we evaluated the proper intensity and application duration needed to achieve the optimal efficacy.

Three intensities (1.3, 4.6, and 8.3 W/cm^2 (unfocused ultrasound, SPTP/SATP; measured by calorimetric method; (33)) and three time periods of ultrasound applications (1, 5, and 10 min) were evaluated. Figure 3 presents the effect of ultrasound application time for ultrasound intensity of 4.6 W/cm^2. As can be seen in Figure 3, the greatest transport enhancements were achieved when ultrasound was applied for 5 min, in comparison to 1 and 10 min for each intensity (the experimental results for 1.3 and 8.3 W/cm^2 yielded the same observation; results not shown). The reduction for the 10 min may be attributed to the acoustic decoupling effect, resulting from the generation of excess cavitation bubbles near the ultrasound probe, thereby reducing propagation of ultrasound wave and decreasing the effective ultrasound intensities the membranes are exposed to.

Figure 4a presents the effect of ultrasound intensities (5 min) on transport enhancement across fetal membranes. In Fig. 4a, there is an increase in fetal membrane permeability with time for passive diffusion (a 2-fold increase); however, the ultrasound intensity effect is much more dominant. The most effective enhancement is achieved during and a short time after ultrasound ("during US") application (for all intensities) in comparison to the base-line ("before US"). When comparing the effect of the different intensities studied for the 5 min application (Fig. 4a), it clearly demonstrates that the most effective intensity for enhanced fetal membrane mass transport is 4.6 W/cm^2 (unfocused ultrasound, SPTP/SATP), which enhances the transport 43-fold relative to the base-line. Since an intensity of 4.6 W/cm^2, 50% duty cycle, for 5 min achieved the greatest enhancement, these values were employed in the following experiments evaluating additional parameters.

Ultrasound Probe Distance

Next we evaluated the optimal probe distance from the fetal membranes. Figure 4b presents an enhancement comparison

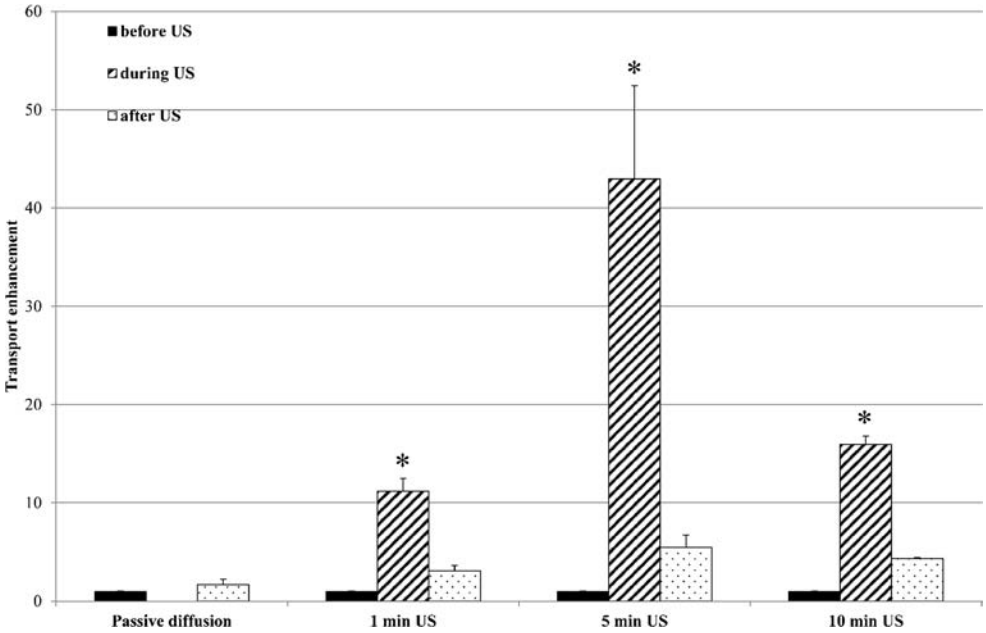

Fig. 3 Ultrasound application time effect on transport enhancement of FITC-Dextran (250 kDa) through post-delivery human fetal membranes *in vitro* (data points represent mean ± standard error (s.e.m.), of 3–5 identically conducted experiments, each from a different biological source; *t*-test – statistically significant *p* values between different parameters are presented on each graph; there is a significant difference (*$p < 0.05$) between each parameter and its passive control).

between 5 and 30 mm probe distances. These distances were evaluated for a future clinical application: 5 mm distance may be suitable for a probe located close to the fetal membranes (this distance is also known to achieve good enhancement results for transdermal application) (33). The 30 mm distance is suitable for a probe located outside the cervix.

The major difference between the transport enhancements for the 5 mm and 30 mm probe distances (43- and 10-fold, respectively) provides information for optimal conditions, and also implies a possible mechanism causing the enhancement. The differences may support the role of cavitational (and the induced acoustic streaming from bubble collapse) effects on the membranes. Cavitational effect is decreased with distance, thus reducing its effect on the membrane permeability. This may explain why increasing the probe distance from the membrane results in lesser enhancement in fetal membranes permeability.

Temperature

In order to eliminate the possibility that mass transport enhancement is attributed to heat generated during insonation, the effect of extremely high temperature (55°C) on mass transport across the fetal membranes was assessed. In order to do so, we performed mass transport experiments where the diffusion cells were placed in a water-filled container at a temperature of 55°C, without insonation. The results are presented in Fig. 4c. As can be seen, fetal membrane exposure to a temperature of 55°C for 5 min resulted in a 7-fold enhancement, while 5 min of insonation resulted in a 43-fold enhancement. Thus the increase in temperature contributes only ~16% (7/43) to the transport enhancement seen for ultrasound. This contribution is even less than 16% when considering that applying ultrasound for 5 min (4.6 W/cm^2) induces much less temperature elevation. This phenomenon is similar to the one seen with skin, where the temperature contributed only 25% of transport enhancement (35).

Ex Vivo Experiments

Based on the *in vitro* experiments, we moved to *ex vivo* experiments on an SD rat model, in order to demonstrate whether the same phenomena occur in a whole amniotic sac (Fig. 1). We first performed mass transport experiments with the model molecule used in the *in vitro* experiments (FITC-Dextran), and later with αFP. αFP was chosen since it is measured clinically during pregnancy in maternal serum or amniotic fluid for the detection of fetal abnormalities (6, 36, 37).

FITC-Dextran Transport Through SD rat Amniotic Sacs

Figure 5a displays the fraction of FITC-Dextran mass released from a rat amniotic sac *vs.* time. The optimal ultrasound parameters determined in the *in vitro* studies were used and compared to passive control (no ultrasound was applied). Ultrasound intensity of 7.7 W/cm^2 (unfocused ultrasound, SPTP/SATP) at a probe distance of 30 mm was also evaluated. As can be seen in Fig. 5a, increasing the distance of the probe can be compensated by increasing the intensity (thus higher ultrasound intensity was also evaluated for its effect on

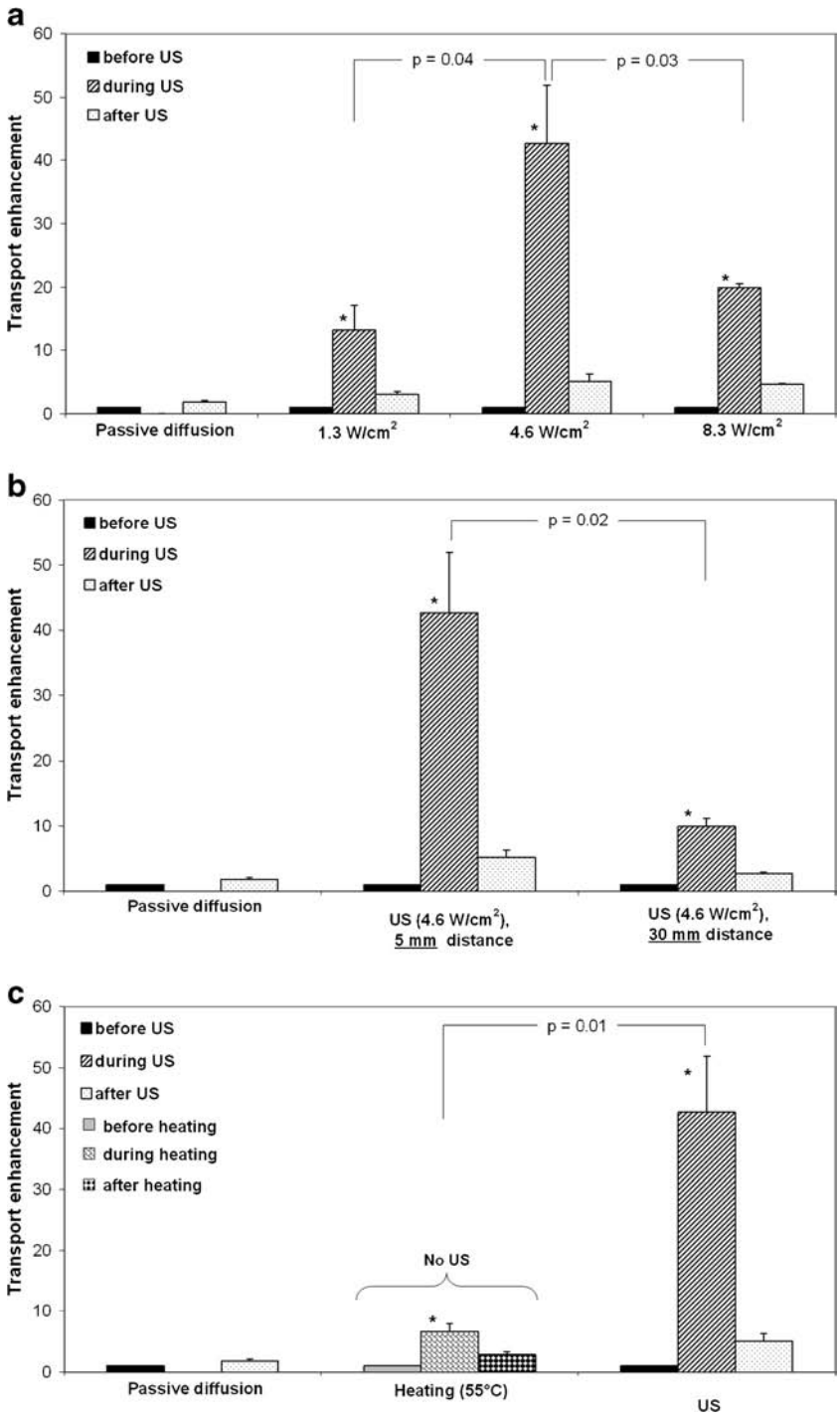

Fig. 4 Different ultrasound parameters' effect on transport enhancement of FITC-Dextran (250 kDa) through post-delivery human fetal membranes *in vitro* (data points represent mean ± standard error (s.e.m.) of 3–5 identically conducted experiments, each from a different biological source; *t*-test – statistically significant *p* values between different parameters are presented on each graph; there is a significant difference (*$p < 0.05$) between each parameter and its passive control). (**a**) Transport enhancement at the three regions of experiment time: before US, during US, and after US application for 5 min at different intensities; duty cycle = 50%; probe distance = 5 mm. (**b**) The effect of ultrasound probe distance from amniotic membrane on transport enhancement. Ultrasound was applied for 5 min at intensity of 4.6 W/cm^2. (**c**) Transport enhancement caused by elevated temperature of 55°C for 5 min (no ultrasound) *vs.* ultrasound application (4.6 W/cm^2) for 5 min (duty cycle = 50%) and passive diffusion.

mass transport), as can be seen in the similar enhancements observed for both ultrasound parameters used.

Figure 5b displays the calculated transport rate for the evaluated parameters and passive diffusion for short and long times after ultrasound application. As was seen in the *in vitro* experiments, the greatest increase in mass transport in *ex vivo* experiments occurs a short time after ultrasound application – as demonstrated by steeper slopes for short time after ultrasound compared to long time after ultrasound (0.91 *vs.* 0.04 for ultrasound intensity of 4.6 W/cm^2); indicating that the transport rate is decreasing after a short time; hence the effect on the fetal membrane permeability is reversible as was shown in the *in vitro* experiments.

αFP Release from a SD Rat Amniotic Sacs

Next, the transport of αFP across SD rat amniotic sacs using our custom *ex vivo* system (Fig. 1a) was assessed; first by

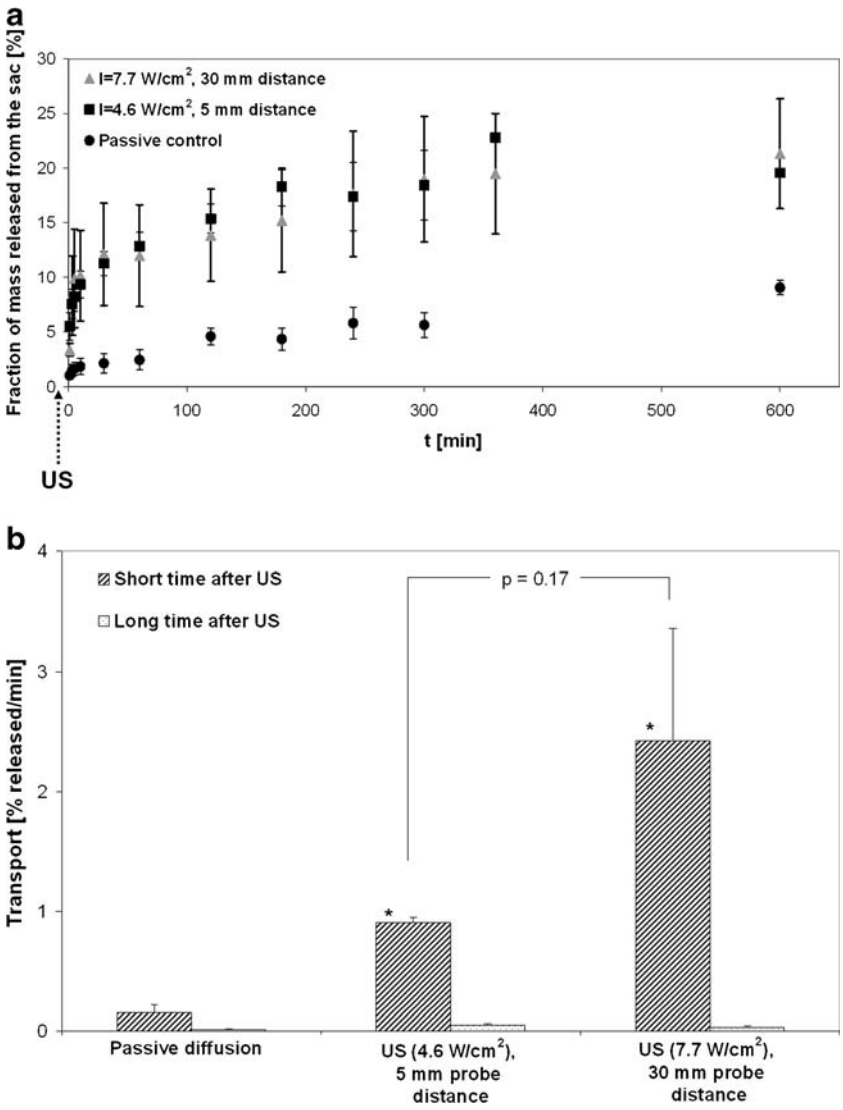

Fig. 5 The enhancement effect of ultrasound on the transport of FITC-Dextran (250 kDa) released from a rat amniotic sac. Data points represent mean ± standard error (s.e.m) of 3–5 identically conducted experiments, each from a different biological source. (**a**) Fraction of mass released from a rat amniotic sac *vs*. time for FITC-Dextran (250 kDa) following ultrasound application for 30 s in a continuous mode, at two intensities (4.6 W/cm^2 and 7.7 W/cm^2); probe distances of 5 mm and 30 mm, respectively, and passive diffusion. The molecule was initially injected into the sac. (**b**) Calculated transport rate (slopes of the fraction of mass released *vs*. time) following ultrasound application for 30 s in a continuous mode, at different intensities (4.6 W/cm^2 and 7.7 W/cm^2), probe distances 5 mm and 30 mm, respectively, and passive diffusion for short (1–5 min) and long time (10–600 min) after ultrasound application. *t*-test: *p*-values are presented on the graph; there is a significant difference (*$p < 0.05$) between each parameter and the passive diffusion).

measuring the base line (passive) transport for 30 min, and only then applying ultrasound for 30 s followed by transport measurements in order to evaluate the ultrasound effect. The results are presented in Fig. 6.

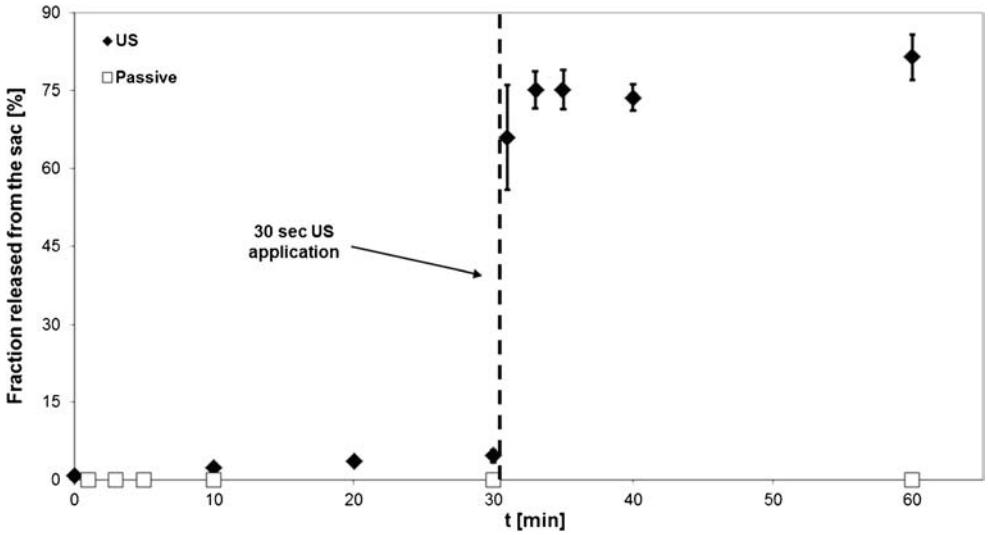

Fig. 6 Fraction of mass released *vs*. time, for αFP (63 kDa) before and after ultrasound application (4.6 W/cm^2; 5 mm probe distance; 30 s application in a continuous mode) and passive diffusion (no ultrasound). Data points represent mean ± standard error (s.e.m.) of 3–5 identically conducted experiments, each from a different biological source.

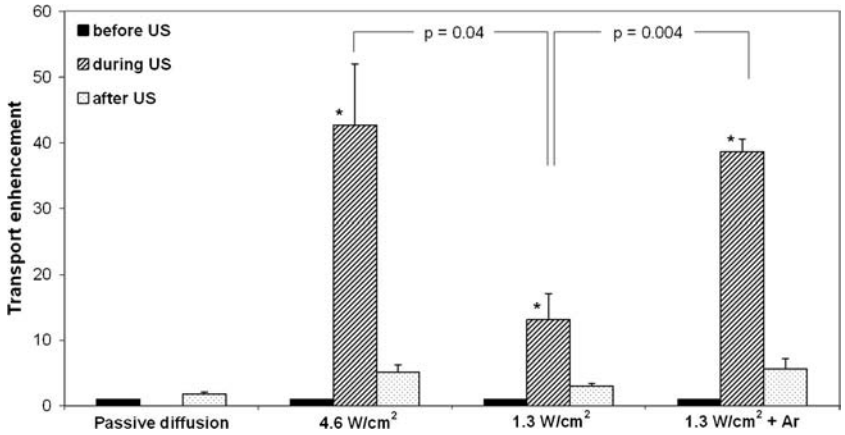

Fig. 7 The effect of continuous Argon (Ar) bubbling into the coupling medium during ultrasound application (1.3 W/cm^2) on transport enhancement of FITC-Dextran (250 kDa) through post-delivery human fetal membranes *in vitro*, compared to ultrasound application without bubbling (1.3 W/cm^2), ultrasound application at a greater intensity (4.6 W/cm^2, no bubbling), and passive diffusion (for all of the ultrasound applications: t = 5 min; duty cycle = 50%; 5 mm probe distance). Data points represent mean ± standard error (s.e.m.) of 3–5 identically conducted experiments, each from a different biological source; *t*-test – statistically significant *p* values between the parameters are presented on the graph; there is a significant difference (*$p < 0.05$) between each parameter and its passive control.

As can be seen in Fig. 6, the base line and the passive αFP fraction released from SD rat amniotic sacs are negligible, while 1 min after insonation it reaches a value of 65% (23-fold of that after 3 min after insonation) of mass released and stays almost constant for the next 30 min. The differences seen between the αFP (Fig. 6) and the FITC-Dextran (Fig. 5a) release profiles (for the FITC-Dextran there is a passive release, while for the αFP there is none) can be attributed to the polarity of αFP (isoelectric point≈4.76, (38)). Previous study (39) has evaluated the permeability of charged and uncharged molecules across the fetal membrane. It was determined that polar molecules with the same molecular mass as nonpolar molecules are less permeable.

The Effect of Argon Gas on Chorioamnion Mass Transport

In order to reduce the ultrasound intensity and further increase the transport enhancement induced by exposure to low intensity ultrasound in order to address safety (40, 41), we decided to increase the number of cavitational events (and induced acoustic streaming, mainly due to bubble collapse) in the coupling medium in contact with chorion by increasing its gas content.

Figure 7 presents the transport enhancement achieved for ultrasound application at lower intensity (than previously used in this study) of 1.3 W/cm^2 with Argon (Ar) bubbling into the

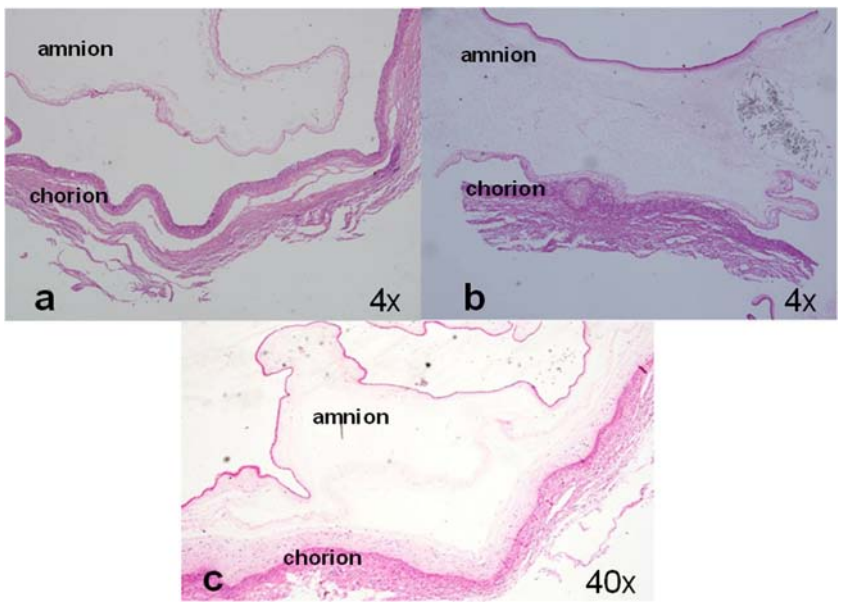

Fig. 8 Representative histological cross-sections of human post-labor fetal membranes following (**a**) passive control, (**b**) ultrasound application (1.3 W/cm^2), and (**c**) ultrasound application (1.3 W/cm^2) + Ar bubbling. Ultrasound was applied for all of the treatments for 5 min at 50% duty cycle, and 5 mm probe distance, *in vitro*.

coupling medium (Ar was chosen since it is known to be a good cavitation enhancer (32, 42)), compared to sonication at the same intensity without bubbling, intensity of 4.6 W/cm^2 (unfocused ultrasound, SPTP/SATP) and passive diffusion. Increasing the gas content of the coupling medium during sonication increases cavitational events within it, which are reflected in the increase of the transport enhancement (39-fold for 1.3 W/cm^2 (unfocused ultrasound, SPTP/SATP) + Ar), in comparison to ultrasound alone (13-fold for 1.3 W/cm^2). Also, these enhancement values (39-fold for 1.3 W/cm^2 + Ar) are similar to those achieved for the higher intensity (43-fold for 4.6 W/cm^2). The greater enhancement achieved with Argon also implies that cavitation is the dominant effect induced by ultrasound.

The results presented so far indicate that ultrasound induced cavitation and its induced streaming are the main mechanisms affecting fetal membrane permeability. The reduction in the enhancing effect, the short term of the effect, and the decoupling phenomena support this conclusion. Thus achieving optimal enhancement effect on fetal membrane permeability can be achieved by intensifying cavitational effects. Due to safety limitations it should be done using low ultrasound intensities as was shown in this study by adding gas content. It may also be achieved by introducing ultrasound contrast agents, which are known to increase the cavitational effect (43).

Safety

Histology Analysis

In order to address other safety issues, we performed histopathology examinations for three treatments: passive diffusion, ultrasound application, and ultrasound application + Ar bubbling. Figure 8 presents representative histology images of cross-sections of fetal membranes following these treatments.

The only histopathology finding was amnion edema (Fig. 8c), seen in one of three repetitions (1.3 W/cm^2 (unfocused ultrasound, SPTP/SATP) + Ar bubbling treatment).

Although there is a need to perform an additional comprehensive safety study in order to eliminate any safety limitations, these preliminary results present a promising noninvasive approach for direct fetal drug delivery and possibly a prenatal diagnostic test.

CONCLUSIONS

Low-frequency ultrasound application enhances the transport of molecules through the fetal membrane in both *in vitro* and *ex vivo* systems in a reversible and transient manner. We suggest that ultrasound's main mechanism of effect on transport enhancement, as in transdermal transport (44–46), is a cavitational (and its induced streaming effect) impact probably on the chorion (which is the rate-limiting membrane for mass transport) (7, 47). These results have the potential to lead to future developments of non-invasive clinical procedures (accessing the fetal membranes via the cervix) for direct fetal drug delivery and possibly also for amniotic fluid sampling for fetal diagnosis.

REFERENCES

1. Aboofazeli R, Zia H, Needham TE. Transdermal delivery of nicardipine: an approach to in vitro permeation enhancement. Drug Deliv. 2002;9(4):239–47.
2. Kushner J, Blankschtein D, Langer R. Heterogeneity in skin treated with low–frequency ultrasound. J Pharm Sci. 2008;97(10):4119–28.
3. Shealtiel L. The effect of Ultrasound on the debridement of chronic wound. PhD thesis. Department of chemical engineering, Ben-Gurion University.
4. Tupker R, Pinnagoda J, Nater J. The transient and cumulative effect of sodium lauryl sulphate on the epidermal barrier assessed by transepidermal water loss: inter-individual variation. Acta Derm Venereol. 1990;70(1):1–5.
5. Gil MM, Akolekar R, Quezada MS, Bregant B, Nicolaides KH. Analysis of Cell-Free DNA in Maternal Blood in Screening for Aneuploidies: Meta-Analysis. Fetal Diagn Ther. 2014.
6. Kost J, Pliquett U, Mitragotri S, Yamamoto A, Langer R, Weaver J. Synergistic effect of electric field and ultrasound on transdermal transport. Pharm Res. 1996;13(4):633–8.
7. Lauterborn W, Kurz T, Geisler R, Schanz D, Lindau O. Acoustic cavitation, bubble dynamics and sonoluminescence. Ultrason Sonochem. 2007;14(4):484–91.
8. Calvin SE, Oyen ML. Microstructure and mechanics of the chorioamnion membrane with an emphasis on fracture properties. Ann N Y Acad Sci. 2007;1101:166–85.
9. Jabareen M, Mallik AS, Bilic G, Zisch AH, Mazza E. Relation between mechanical properties and microstructure of human fetal membranes: an attempt towards a quantitative analysis. Eur J Obstet Gynecol Reprod Biol. 2009;144:S134–41.
10. Shuster S, Black MM, McVitie E. The influence of age and sex on skin thickness, skin collagen and density. Br J Dermatol. 1975;93:639–43.
11. Kost J, Wolloch L. Ultrasound in percutaneous absorption. In: Touitou E, Barry BW, editors. Enhancement in drug delivery. Boca Raton: CRC Press; 2006. p. 317–30.
12. Azagury A, Khoury L, Enden G, Kost J. Ultrasound mediated transdermal drug delivery. Adv Drug Deliv Rev. 2013.
13. Lavon I, Kost J. Ultrasound and transdermal drug delivery. Drug Discov Today. 2004;9(15):670–6.
14. Prausnitz MR, Mitragotri S, Langer R. Current status and future potential of transdermal drug delivery. Nat Rev Drug Discov. 2004;3(2):115–24.
15. Fang J, Fang C, Sung K, Chen H. Effect of low frequency ultrasound on the in vitro percutaneous absorption of clobetasol 17-propionate. Int J Pharm. 1999;191(1):33–42.
16. Bommannan D, Okuyama H, Stauffer P, Guy RH. Sonophoresis. I. The use of high-frequency ultrasound to enhance transdermal drug delivery. Pharm Res. 1992;9(4):559–64.
17. Boucaud A, Machet L, Arbeille B, Machet M, Sournac M, Mavon A, et al. In vitro study of low-frequency ultrasound-enhanced

transdermal transport of fentanyl and caffeine across human and hairless rat skin. Int J Pharm. 2001;228(1):69–77.
18. Mitragotri S, Kost J. Transdermal delivery of heparin and low-molecular weight heparin using low-frequency ultrasound. Pharm Res. 2001;18(8):1151–6.
19. Mutoh M, Ueda H, Nakamura Y, Hirayama K, Atobe M, Kobayashi D, et al. Characterization of transdermal solute transport induced by low-frequency ultrasound in the hairless rat skin. J Control Release. 2003;92(1):137–46.
20. Tachibana K, Tachibana S. Transdermal delivery of insulin by ultrasonic vibration. J Pharm Pharmacol. 1991;43(4):270–1.
21. Mitragotri S, Blankschtein D, Langer R. Ultrasound-mediated transdermal protein delivery. Science. 1995;269(5225):850–3.
22. Mitragotri S, Blankschtein D, Langer R. Transdermal drug delivery using low-frequency sonophoresis. Pharm Res. 1996;13(3):411–20.
23. Katz NP, Shapiro DE, Herrmann TE, Kost J, Custer LM. Rapid onset of cutaneous anesthesia with EMLA cream after pretreatment with a new ultrasound-emitting device. Anesth Analg. 2004;98(2):371–6.
24. Kost J, Mitragotri S, Gabbay RA, Pishko M, Langer R. Transdermal monitoring of glucose and other analytes using ultrasound. Nat Med. 2000;6(3):347–50.
25. Mitragotri S, Coleman M, Kost J, Langer R. Transdermal extraction of analytes using low-frequency ultrasound. Pharm Res. 2000;17(4):466–70.
26. Chuang H, Taylor E, Davison TW. Clinical evaluation of a continuous minimally invasive glucose flux sensor placed over ultrasonically permeated skin. Diabetes Technol Ther. 2004;6(1):21–30.
27. Lee S, Nayak V, Dodds J, Pishko M, Smith NB. Glucose measurements with sensors and ultrasound. Ultrasound Med Biol. 2005;31(7):971–7.
28. Schaefer H, Redelmeier TE. Skin barrier. Principles of Percutaneous Absorption. Arzneimittel-Forschung. 1997;47(2):228–9.
29. Johnson-Hopson NC, Artlett IMC. Evidence against the long-term persistence of fetal DNA in maternal plasma after pregnancy. Hum Genet. 2002;111(6):575–5.
30. Lavon I, Grossman N, Kost J, Kimmel E, Enden G. Bubble growth within the skin by rectified diffusion might play a significant role in sonophoresis. J Control Release. 2007;117(2):246–55.
31. Nishida Y, Yoshida S, Li HJ, Higuchi Y, Takai N, Miyakawa I. FTIR spectroscopic analyses of human placental membranes. Biopolymers. 2001;62(1):22–8.
32. Wolloch L, Kost J. The importance of microjet vs shock wave formation in sonophoresis. J Control Release. 2010;148(2):204–11.
33. Terahara T, Mitragotri S, Kost J, Langer R. Dependence of low-frequency sonophoresis on ultrasound parameters; distance of the horn and intensity. Int J Pharm. 2002;235(1):35–42.
34. Polat BE, Deen WM, Langer R, Blankschtein D. A physical mechanism to explain the delivery of chemical penetration enhancers into skin during transdermal sonophoresis—Insight into the observed synergism. J Control Release. 2012;158:250–60.
35. Merino G, Kalia YN, Delgado-Charro MB, Potts RO, Guy RH. Frequency and thermal effects on the enhancement of transdermal transport by sonophoresis. J Control Release. 2003;88(1):85–94.
36. Zderic V, Clark JI, Vaezy S. Drug delivery into the eye with the use of ultrasound. J Ultrasound Med. 2004;23(10):1349–59.
37. Traitel T, Kost J, Lapidot SA. Modeling ionic hydrogels swelling: characterization of the non–steady state. Biotechnol Bioeng. 2003;84(1):20–8.
38. Watabe H. Purification and chemical characterization of α-fetoprotein from rat and mouse. Int J Cancer. 1974;13:377–88.
39. Bajoria R, Fisk NM. Permeability of human placenta and fetal membranes to thyrotropin-stimulating hormone *in vitro*. Pediatr Res. 1998;43:621–8.
40. Dugoff L, Hobbins JC, Malone FD, Porter TF, Luthy D, Comstock CH, et al. First-trimester maternal serum PAPP-A and free-beta subunit human chorionic gonadotropin concentrations and nuchal translucency are associated with obstetric complications: a population-based screening study (the FASTER Trial). Obstet Gynecol. 2004;191(4):1446–51.
41. Barry B. Lipid-protein-partitioning theory of skin penetration enhancement. J Control Release. 1991;15(3):237–48.
42. Mason TJ. Chemistry with ultrasound. Amsterdam: Elsevier Science Pub. Co.; 1990. p. 8–10.
43. Park D, Yoon J, Park J, Jung B, Park H, Seo J. Transdermal drug delivery aided by an ultrasound contrast agent: an in vitro experimental study. Open Biomed Eng J. 2010;4:56–62.
44. Tezel A, Mitragotri S. Interactions of inertial cavitation bubbles with stratum corneum lipid bilayers during low-frequency sonophoresis. Biophys J. 2003;85(6):3502–12.
45. Tang H, Wang CCJ, Blankschtein D, Langer R. An investigation of the role of cavitation in low-frequency ultrasound-mediated transdermal drug transport. Pharm Res. 2002;19(8):1160–9.
46. Tezel A, Sens A, Mitragotri S. Investigations of the role of cavitation in low–frequency sonophoresis using acoustic spectroscopy. J Pharm Sci. 2002;91(2):444–53.
47. Kopelman D, Papa M. Magnetic resonance–guided focused ultrasound surgery for the noninvasive curative ablation of tumors and palliative treatments: a review. Ann Surg Oncol. 2007;14(5):1540–50.